20th Australasian Fluid Mechanics Conference
Perth, Australia
5-8 December 2016

Influence of Non-gray Participating Media and Wall Surface on Turbulent Natural Convection Heat Transfer in Cubic Cavity

T. Kogawa[1], J. Okajima[2], A. Komiya[2], and S. Maruyama[2]

[1]Department of Mechanical Engineering
Tohoku University, Sendai Miyagi, Aoba Aramaki 6-6, Japan

[2]Instituet of Fluid Science
Tohoku University, Sendai, Miyagi, Aoba Katahira 2-1-1, Japan

Abstract

In this study, influences of participating media and wall surfaces on heat transfer of turbulent natural convection of a differentially heated cubic cavity were investigated. Coupled calculation of the convective and radiative heat transfers was conducted using the large eddy simulation (LES). To calculate the radiative heat transfer, the Radiation element method by the ray emission model (REM^2) was utilized. The non-gray participating media was modelled by the full spectrum *k*-distribution (FSK) model, which accounts for the wavelength dependency of the absorption coefficient. Changing emissivity, specular, and diffuse reflectance of surrounding walls, the effect of the wall surface was studied. The calculation conditions with black body, specular and diffuse surface were investigated. When the surrounding walls were black bodies, flow instability increased strongly. Contrary to the black body conditions, the flow instabilities under the specular and diffuse surface conditions were weak and the radiative heat transfers from heated wall were almost same with the specular and diffuse surfaces. To investigate the influence of the participating media on the heat transfer, the concentration of the participating media was changed. When the concentration of the participating media was higher, the flow instability was enhanced while convective heat transfer was not affected.

Introduction

A natural convection is induced by a buoyant force coming from a density difference of a fluid. Therefore, the natural convection is generated by only a potential energy and this phenomenon does not need an external energy while a forced convection requires the external energy. Natural convection can be observed in both of the small and large scale. In the large-scale natural convection, the buoyant force is adding up because of its huge space, and the driving force is much higher than that of the small-scale natural convection. Because of this huge driving force, flow instability is facilitated and a turbulent flow is generated. The large-scale natural convection has been utilized in ventilation of building, exhausting gas, combustion chamber and nuclear power plant systems for recent decades. If strategies and systems using the large-scale natural convection could be used effectively, energy consumption and emission of carbon dioxide could be significantly saved. The large-scale natural convection can be divided in two type flows at low (280-330 K) and high (350–400 K) temperature conditions.

In the low temperature condition, the large-scale natural convection is frequently used in the ventilation method of the building. In the ventilation method, building structure becomes an important factor to design the system because the building structure affected both of convective and radiative heat transfers drastically. Xin et al., [7] investigated a turbulent natural convection for air inside a cubic cavity with the Rayleigh number of 1.5×10^9 conducting the direct numerical simulation (DNS). They indicated that emitted radiation from the surrounding wall is an important factor to determine velocity boundary layers developing around surrounding walls.

In high temperature condition, the large-scale natural convection is applied and observed in an exhausting gas and combustion systems. When fluid temperature becomes higher, the radiation from a gas affects a total heat transfer. Furthermore, in the exhaust gas and combustion system, the water vapour and carbon dioxide which emits and absorb the radiation are exhausted extremely due to the chemical reaction. Because of these reasons, to evaluate the large-scale natural convection at high temperature condition, the participating media effect on the heat transfer has to be investigated. The effects on the laminar natural convection have been investigated adequately using the gray gas model [2]. The coupling simulation with non-gray gas model has also been analysed. Lari et al. [3] applied the FSK [5] and investigated the participating media effect on the heat transfer at exhaust gas condition. The effect of the participating media on the turbulent natural convection heat transfer has also been studied, Fusegi et al. [1] calculated the turbulent natural convection of the square cavity for combustion gas case and they evaluated the heat transfer and iso-surface of the temperature.

As mentioned above, the natural convection with coupling the radiative heat transfer has been analysed at both of the low temperature and high temperature conditions. In low temperature condition, the wall condition becomes important to determine the heat transfer [7]. On the other hand, in the high temperature condition, the effect of the participating media becomes important factor on the natural convection heat transfer. To evaluate the turbulent natural convection quantitatively, wall boundary condition and participating media effect on the turbulent natural convection have to be investigated. However, the discussion about the radiative properties of the wall and effect of the participating media was limited because coupled simulation with radiative heat transfer is time consuming and complicated. The aim of the present study is to investigate the influence of the wall condition and participating media on the heat and fluid flow characteristics of the turbulent natural convection. Changing the emissivity, specular and diffuse reflectance, the effect of the wall boundary condition was evaluated. Varying the partial pressure of the participating media gas, H_2O and CO_2, the effect of the participating media was also investigated with the atmospheric and exhaust gas cases.

Calculation Method

Figure 1 shows the calculation model used in this study. The calculation model was a cubic cavity, which has the heated and cooled wall maintained by the uniform temperature. The working fluid was air. Air contained the H_2O and CO_2 as a participating

media. The isothermal walls were assumed to be a black bodies. The radiative properties of the surrounding walls (top, bottom, front, and back walls) were varied with each calculation condition. The precise calculation condition for the boundary condition of the walls and the partial pressure of the participating media were discussed later.

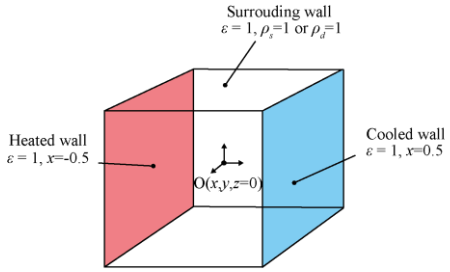

Figure 1 Calculation model of the cubic cavity

The governing equations; continuity, /N-S, energy, and radiative heat transfer equation (RTE) used in present study can be written as follows:

$$\frac{\partial \overline{u_k}}{\partial x_k} = 0, \tag{1}$$

$$\frac{\partial \overline{u_i}}{\partial t} + \overline{u_j}\frac{\partial \overline{u_i}}{\partial x_j} = -\frac{\partial \overline{p}}{\partial x_i} + \frac{Pr}{\sqrt{Ra}}\frac{\partial}{\partial x_j}\frac{\partial \overline{u_i}}{\partial x_j} - \frac{\partial}{\partial x_j}\tau_{ij} + Pr\left(\overline{\theta} - \theta_{ave}\right)\delta_{i2}, \tag{2}$$

$$\frac{\partial \overline{\theta}}{\partial t} + \overline{u_j}\frac{\partial \overline{\theta}}{\partial x_j} = \frac{1}{\sqrt{Ra}}\frac{\partial}{\partial x_j}\frac{\partial \overline{\theta}}{\partial x_j} + q_t - \frac{L^2}{\sqrt{Ra}k\Delta T}\nabla\cdot\overline{q_r}, \tag{3}$$

$$\frac{d\overline{I_\lambda}(\vec{r},\vec{s})}{ds} = k_\lambda\left[-\overline{I_\lambda}(\vec{r},\vec{s}) + \overline{I_{b\lambda}}(T)\right]. \tag{4}$$

Continuity equation, N-S equation and energy equation are made dimensionless. Here, u_i [-], x_i [-], t [-], p [-], θ [-] are dimensionless velocity, distance, time, pressure, and temperature. Pr [-], Ra [-], ΔT [K], L [m], κ [W m^{-1} K^{-1}], q_r [W m^{-2}], and δ_{ij} [-] are Prandtl number, Rayleigh number, temperature difference of the cavity, cavity length, thermal conductivity, radiative heat flux, and function of the delta. τ [-] and q_t [-] are turbulent stress and turbulent heat flux modelled by LES. I [W m^{-2} sr^{-1} m^{-1}], s [m], $\vec{r}$ [m], $\vec{s}$ [-], and k [m^{-1}] are radiative intensity, optical path, unit position vector, unit vector of the radiative intensity, and absorption coefficient of the participating media. The each term of the governing equations was filtered by the one-third power of the gird volume. The buoyant force was considered by the Boussinesq approximation. κ and Pr were determined from the bulk temperature of the air.

The turbulent stress and heat flux modelled by LES can be written as follows:

$$\tau_{ij} = -2\nu_{SGS}\overline{S_{ij}} + \frac{1}{3}\tau_{kk}\delta_{ij}, \tag{5}$$

$$q_t = -\alpha_{SGS}\frac{\partial \overline{\theta}}{\partial x_j}, \tag{6}$$

Here, S_{ij} [-] is strain tensor. ν_{SGS}, [-] and α_{SGS} [-] represent the turbulent kinematic viscosity and thermal diffusivity of SGS. ν_{SGS} was calculated by the Vreman model [6] as a LES model to switch the laminar and turbulent flow adequately. α_{SGS} was modelled by the constant turbulent Prandtl number Pr_t of 0.4.

The divergence of the radiative heat flux, which appears in the energy equation, is calculated using the radiative intensity as follows,

$$\nabla\cdot q_r = \int_0^\infty\left(k_\lambda\left(4\pi\overline{I_{b\lambda}}(\vec{r}) - \int_{4\pi}\overline{I_\lambda}(\vec{r},\vec{s})d\Omega\right)\right)d\lambda. \tag{7}$$

In the boundary of the surrounding walls, the adiabatic boundary condition was applied. The energy balance between the convective heat transfer and radiative heat transfer is consisted. The temperature gradient was calculated using the radiative heat flux of the boundary as follows:

$$\frac{\partial \overline{\theta}}{\partial x_n} = -\frac{L}{k\Delta T}q_r, \tag{8}$$

$$q_r = \int_0^\infty\left(\varepsilon_w\left(\pi\overline{I_{b,w,\lambda}}(\vec{r}_w) - \int_{\vec{n}\cdot\vec{s}<0}\overline{I_\lambda}(\vec{r}_w,\vec{s})\left|\vec{n}\cdot\vec{s}\right|d\Omega\right)\right)d\lambda. \tag{9}$$

Here, ε_w [-], Ω [sr], λ [μm] are emissivity of the boundary, solid angle, and wavelength respectively.

To calculate the radiative heat flux of the participating media and boundary, REM^2 proposed by Maruyama et al. [4] was applied. Using REM^2, the RTE is integrated over the area where radiative intensities pass and the divergence of the radiative heat flux and radiative heat flux of the boundary can be calculated as follows:

$$\nabla\cdot q_r = \frac{\int_0^\infty\left(Q_{T,i} - \sum_{j=1}^{N}\varepsilon_i F^E_{i,j,l}Q_{J,j}\right)dl}{dV}, \tag{10}$$

$$q_r = \frac{\int_0^\infty\left(Q_{T,i} - \sum_{j=1}^{N}\varepsilon_i F^E_{i,j,l}Q_{J,j}\right)dl}{dA}. \tag{11}$$

Here, $Q_{T,i}$ [W], ε_i [-], $F^E_{i,j,l}$ [-], $Q_{J,i}$ [W], dV [m^3], and dA [m^2] are emission power, emissivity of the radiation element, extinction view factor, power from the other radiation element, volume of the radiation element, and area of the surface radiation element respectively.

To calculate the radiative heat flux, wavelength dependency of the absorption coefficient was considered using FSK model [5]. In FSK, the k-distribution against the cumulative function g [-] is determined and the RTE and boundary condition of the radiative heat transfer can be transformed from the wavelength dependency to the cumulative function dependency as follows:

$$\frac{d\overline{I_g}(\vec{r},\vec{s})}{ds} = k_g\left(-\overline{I_g}(\vec{r},\vec{s}) + \overline{I_{b,g}}(T)\right), \tag{12}$$

$$I_{w,g} = \varepsilon_w a(T_w,T,g)\overline{I_{b,w,g}} + \frac{(1-\varepsilon_w)}{\pi}\int_{\vec{n}\cdot\vec{s}<0}\overline{I_g}(\vec{r}_w,\vec{s})\left|\vec{n}\cdot\vec{s}\right|d\Omega. \tag{13}$$

Here, a [-] is weight function for the boundary. In this study, the temperature difference of the cavity was small and a can be assumed to be 1. The absorption coefficient distribution against the wavelength was calculated from the line by line method. To determine the cumulative function, the bulk temperature of the cavity and reference pressure of 1 atm were used. To calculate the absorption coefficient from the k-distribution, 12 Gauss quadrature points were selected.

The total fluid grid number were 172×172×172 in the x, y, and z directions, respectively. To capture the turbulence by grid scale, the grid sizes around the isothermal walls and surrounding walls had smallest value. The grid size in the x, y, and z directions varied from 1.0×10^{-4} to 8.0×10^{-3}. In this case, the optical thickness was thin, and the radiation interaction with the fluid was small. Therefore, the radiation grid number can be smaller than that of the fluid grid. A non-uniform radiation grid was also adopted in the x direction to have the fine mesh around

isothermal walls. The total radiation grid number were 30×20×20. The grid size of x direction varied from 1.0×10^{-3} to 5.0×10^{-2} dimensionless distance while grid sizes of y and z directions had uniform dimensionless distance of 5.0×10^{-2}.

The governing equations of N-S equation and energy equation were discretized by the finite volume method using the collocated grids. Second order total variation diminishing (TVD) schemes were utilized for the convective terms. The solution advance obeys the fully implicit method. Pressure was predicted by the Pressure-implicit with splitting of operators (PISO) method. The time step was accompanied by the Courant-Friedrichs-Lewy (CFL) condition, with a number of 0.35. To couple the convective heat transfer and radiative heat transfer, the radiative heat flux was updated at the interval of 0.2 dimensionless time. Before starting the fluid calculations, the extinction view factors, which are needed for the calculation of the radiative heat transfer, were calculated and stored in the computational memories.

Results and Discussion

Influence of the boundary condition of the wall

To analyze the influence of the wall condition on the turbulent natural convection, the boundary condition of the surrounding wall (top, bottom, front, and back walls) of the cubic cavity was changed. Table 1 shows the boundary condition of the surrounding walls. The wall conditions; black body, specular surface, and diffuse surface were evaluated. The isothermal walls of the heated and cooled wall were maintained at 307.5 K and 292.5 K respectively. The bulk of the temperature was 300 K. The cavity length was 1 m and the *Ra* of the cubic cavity was 1.5×10^{9}. The working fluid was atmospheric gas and this gas contained H_2O of 1.75×10^{-2} atm and CO_2 of 3.8×10^{-4} atm. The total pressure was 1 atm.

Calculation condition	Emissivity ε	Specular reflectance ρ_S	Diffuse reflectance ρ_D
Black cond.	1	0	0
Specular cond.	0	1	0
Diffuse cond.	0	0	1

Table 1 Boundary condition of the surrounding walls

To discuss of the wall boundary condition effect, the calculation results for the non-radiation case was also investigated. In, "non-radiation case", the emissivity of the surrounding wall was set to 0 and the participating media was concerned as a transparent media.

Figure 2 shows the temperature distribution of each calculation condition. In the natural convection of the enclosure, the temperature stratification is generated inside the cavity in general. As can be seen in the black condition, the temperature stratification was restrained compared to the non-radiation case. This results means the thermal diffusion for the vertical direction increased significantly. In black body condition, the horizontal convection was created by the temperature difference, which was made by the radiation absorption and emission on the top and bottom walls. As a result of the strong horizontal convection, flow circulation in the cavity increased thermal diffusion for the vertical direction. Therefore, the temperature stratification of the black body condition was not observed.

Contrary to the black body condition, the temperature stratifications of the specular and diffuse surface conditions had similar result with that of the non-radiation case. Even though the horizontal convection was generated, the flow circulation enhanced by the gas radiation was weaker than that of the black body condition and the temperature stratifications in both of the specular and diffuse surface were similar distribution of the non-radiation case. However, small variation was observed compared to the non-radiation case and this result implies that gas radiation had influence on the thermal diffusion of the vertical direction.

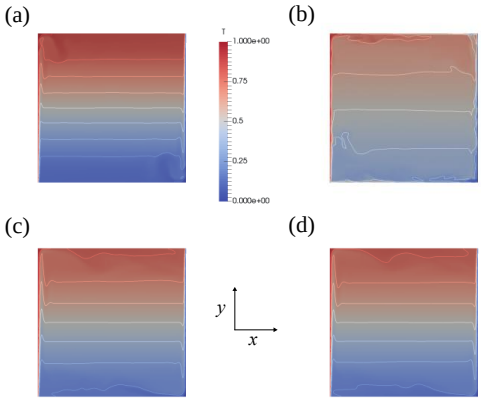

Figure 2 Temperature distributions of each calculation condition at z=0 plane, (a) Non-radiation, (b) Black body, (c) Specular surface, (d) Diffuse surface

To evaluate the influence of the wall conditions on the total heat transfer, average total Nusselt number (*Nu*) was compared in each calculation condition. The average total *Nu* from heated wall was investigated using the equation written as follows:

$$\overline{Nu_{total}} = \overline{Nu_{conv}} + \overline{Nu_{rad}} = \int_{-0.5}^{0.5} \left.\frac{\partial \bar{q}}{\partial x}\right|_{x=-0.5} dy + \int_{-0.5}^{0.5} \frac{\bar{q}_r L}{/ \mathrm{D}T} dy \qquad (14)$$

Here, average total *Nu* is summation of the average convective and radiative *Nu*. Each average *Nu* was integrated with the centerline of the heated wall. Table 2 shows the average *Nu* from heated wall of each calculation condition.

Calculation condition	Total *Nu*	Convective *Nu*	Radiative *Nu*
Non-radiation + $\sigma\left(T_h^4 - T_c^4\right)$	297.3 (100 %)	62.94 (100 %)	234.4 (100 %)
Black body	191.6 (64.4 %)	58.52 (93.0 %)	133.1 (56.8 %)
Specular surface	275.0 (92.5 %)	57.8 (91.8 %)	217.2 (92.7%)
Diffuse surface	274.3 (92.3 %)	58.43 (92.8 %)	215.9 (92.2 %)

Table 2 Heat transfer from heated wall

To compare the heat transfer quantitatively, the heat transfer of the non-radiation case was assumed to be 100 %. In the non-radiation case, the average radiative *Nu* was added by estimating the radiative heat flux if isothermal walls are assumed to be black bodies.

Comparing the heat transfer of the black body condition, the average radiative *Nu* was lower than that of the non-radiation case and about decreasing amounts of 43 % was estimated. However, the average convective *Nu* was similar to that of the non-radiation case. In the black body condition, the acceleration of the vortex generation was observed and the convective heat transfer enhancement by the turbulent mixing will be expected. Nevertheless, the increasing of average convective *Nu* was not estimated. This result implies the turbulent instability by the radiation effect in the black body condition did not affect the convective heat transfer. The velocity gradient around the heated wall was same distribution in all calculation conditions although the different flow patterns could be found in the outer region of the velocity boundary layer. This result indicates that convection

around heated wall did not vary by the radiation effect and the average convective *Nu* did not change drastically.

In both of specular and diffuse surface cases, the average radiative *Nu* was slightly reduced compared to the non-radiation case, the reduced amounts of the average radiative *Nu* were about 7-8 %. This slight reducing was caused by the radiation absorption by the low concentration of the participating media. The average convective *Nu* in both surface cases had similar values of the non-radiation case.

Influence of the participating media

To evaluate the influence of the participating media on the turbulent natural convection, the partial pressures of the H_2O and CO_2 were varied. The considered calculation conditions were atmospheric and exhaust gas cases. Table 3 shows the calculation condition of both cases. In two calculation cases, *Ra* was constant value of 1.5×10^9. To have same *Ra* of both conditions, the cavity length *L* was varied. The temperatures of the heated and cooled walls were maintained at 307.5 K, 292.5 K, and 357.5 K, 342.5 K with the atmospheric and exhaust gas cases respectively. The total pressure of both conditions was 1 atm. To discuss only the gas radiation effect and exclude the surface radiation effect, the surrounding walls were set to the diffuse surface.

Calculation condition	p_{H_2O} [atm]	p_{H_2O} [atm]	T_0 [K]	L [m]
Atmospheric gas	1.75×10^{-2}	3.80×10^{-4}	300	1.0
Exhaust gas	1.00×10^{-1}	2.00×10^{-1}	350	1.3

Table 3 Calculation condition of the participating media

Figure 3 shows the temperature distribution of the atmospheric and exhaust gas conditions. As can be seen this figure, the temperatures stratification of the exhaust gas condition was restrained in the exhaust gas condition. In the exhaust gas condition, the horizontal convection was strengthened due to the absorption of the radiation and the flow circulation enhanced the thermal diffusion of the vertical direction.

Table 4 shows the heat transfer from heated wall in each calculation conditions. Compared to the atmospheric condition, the average radiaitve *Nu* becomes much higher in the exhaust gas condition because of its high temperature situation. The average convective *Nu* for both gas conditions were similar values although the enhancement of the flow instability was observed in the exhaust gas case. This tendency can be explained by same reason as discussed in the black body condition for the atmospheric gas condition.

Conclusions

In this study, the influence of the wall condition and participating media on the turbulent natural convection heat transfer in the cubic cavity has been investigated. Using the coupled simulation between convective heat transfer and radiative heat transfer, following conclusions were obtained as in this study.

1. The temperature stratification of black body condition was restrained because of the enhancement of the flow circulation by the surface radiation.
2. The black body wall significantly influenced the radiative heat transfers.
3. In the exhaust gas condition, temperature distribution was similar to that of the black body condition by the enhancement of the flow circulation.
4. Enhancement of the flow instability, which was seen in the black body condition and exhaust gas condition, did not affect the convective heat transfer.

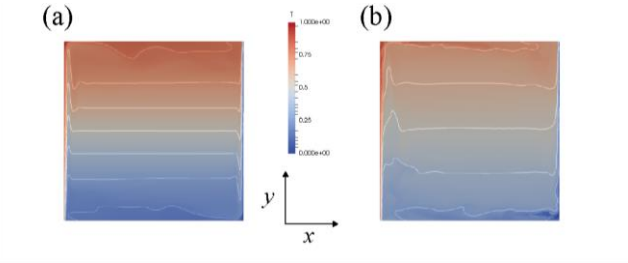

Figure 3 Temperature distributions at z=0 plane, (a) Atmospheric gas, (b) Exhaustst gas

Calculation condition	Total *Nu*	Convective *Nu*	Radiative *Nu*
Atmospheric gas	274.3	58.43	215.9
Exhaust gas	379.8	57.17	322.6

Table 4 Heat transfer from heated wall

Acknowledgments

This research was supported by Grant-in-Aid for JSPS Fellows number 15J04088. This research used computational resources of the SGI UV2000 provided by the Institute of Fluid Science, Tohoku University.

References

[1] T. Fusegi, B. Farouk, Laminar and turbulent natural convection-radiation interaction in a square enclosure filled with a nongray gas, Numerical Heat Transfer, Part A, **15**, 1988, 303-322.

[2] K. Lari, M. Baneshi, S. A. G. Nassab, A. Komiya, S. Maruyama, Combined heat transfer of radiation and natural convection in a square cavity containing participating gases, International Journal of Heat and Mass Transfer, **54**, 2011, 5087-5099.

[3] K. Lari, M. Baneshi, S. A. G. Nassab, A. Komiya, S. Maruyama, Numerical Study of Non-Gray Radiation and Natural Convection Using the Full-Spectrum k-Distribution Method, *Numerical Heat Transfer, Part A: Applications*, **61**, 2012, 61-84.

[4] S. Maruyama, T. Aihara, Radiation heat transfer of arbitrary three-dimensional absorbing, emitting and scattering media and specular and diffuse surfaces, Journal of Heat Transfer, **119**, 1997, 129-136.

[5] M. F. Modest, H. Zhang, The Full-Spectrum Correlated-k Distribution for Thermal Radiation From Molecular Gas-Particulate Mixtures, Journal of Heat Transfer, **124**, 2003, 30-38.

[6] A. W. Vreman, An eddy-viscosity subgrid-scale model for turbulent shear flow: Algebraic theory and applications, Physics of Fluids, **16**, 2004, 3670-3681.

[7] S. Xin, J. Salat, P. Joubert, A. Sergent, F. Petbit, P. L. Quere, Resolving the stratification discrepancy of turbulent natural convection in differentially heated air-filled cavities. Part Ⅲ full convection-conduction-surface radiation coupling, International Journal of Heat and Fluid Flow, **42**, 2013, 33-48.